FRIEDRICH-ALEXANDER-UNIVERSITÄT ERLANGEN-NÜRNBERG
INSTITUT FÜR INFORMATIK (MATHEMATISCHE MASCHINEN UND DATENVERARBEITUNG)

Lehrstuhl für Informatik 10 (Systemsimulation)

On the Construction of Prolongation Operators in Multigrid

Roman Wienands and Harald Köstler

Lehrstuhlbericht 09-4

On the Construction of Prolongation Operators for Multigrid

Roman Wienands[*]and Harald Köstler[†]

Abstract

We discuss a general framework for the construction of prolongation operators for multigrid methods and show that classical matrix-dependent transfers like black box prolongation can be recovered as special cases. The approach can be used both in a geometric and in a pure algebraic multigrid setting and it allows for a simple and efficient implementation and parallelization in 2D and 3D. We present numerical results for several two- and three-dimensional diffusion problems including jumping coefficients and apply our method to a real-world three-dimensional image segmentation problem arising in medical applications.

1 Introduction

Multigrid methods [1, 2, 3, 5, 8, 9, 12, 13, 15] are widely accepted as the most efficient algorithms for the numerical solution of elliptic boundary value problems (BVPs). Assuming a proper discretization of the BVP under consideration one usually ends up with a linear system

$$\mathbf{A}\mathbf{u} = \mathbf{f}$$

with matrix $\mathbf{A} \in \mathbb{R}^{n\times n}$, right-hand side vector $\mathbf{f} \in \mathbb{R}^n$, and solution vector $\mathbf{u} \in \mathbb{R}^n$. Multigrid algorithms are based on two main principles: Firstly, it is well-known that classical relaxation methods (like Jacobi and Gauss-Seidel relaxation) have a strong error smoothing effect (*smoothing principle*). Secondly, a smooth error term can be well approximated on a coarser grid saving a substantial amount of computational work (*coarse grid correction principle*). These two principles suggest the following structure of a two-grid cycle:

- Pre-smoothing: Perform ν_1 steps of an iterative relaxation method $\mathbf{S} \in \mathbb{R}^{n\times n}$ on the fine grid.

[*] wienands@math.uni-koeln.de

[†] harald.koestler@informatik.uni-erlangen.de

- Coarse grid correction:
  - compute the defect $\mathbf{d} = \mathbf{f} - \mathbf{A}\bar{\mathbf{u}}$ of the current fine grid approximation $\bar{\mathbf{u}}$,
  - restrict the defect to the coarse grid using a restriction operator $\mathbf{R} \in \mathbb{R}^{n \times n_c}$,
  - solve the coarse grid defect equation $\mathbf{A}_c\mathbf{v}_c = \mathbf{R}\mathbf{d} = \mathbf{d}_c$ based on a coarse approximation $\mathbf{A}_c \in \mathbb{R}^{n_c \times n_c}$ for the given fine grid matrix $\mathbf{A}$,
  - interpolate the obtained error correction to the fine grid with the help of a prolongation operator $\mathbf{P} \in \mathbb{R}^{n_c \times n}$,
  - add the interpolated correction to the current fine grid approximation.
- Post-smoothing: Perform ν_2 steps of an iterative relaxation method on the fine grid.

The resulting two-grid error transformation matrix reads:

$$\mathbf{M} = \mathbf{S}^{\nu_2}\left(\mathbf{I} - \mathbf{P}\mathbf{A}_c^{-1}\mathbf{R}\mathbf{A}\right)\mathbf{S}^{\nu_1}$$

with fine grid identity matrix $\mathbf{I} \in \mathbb{R}^{n \times n}$. Instead of an exact solution of the coarse grid equation, it can of course be solved by a recursive application of the two-grid iteration, yielding a multigrid method.

Now, the quality of multigrid methods crucially depends on an efficient interplay between the smoothing operator $\mathbf{S}$ and prolongation $\mathbf{P}$. More precisely, the range of $\mathbf{S}$ should be sufficiently well represented in the range of $\mathbf{P}$. To illustrate this condition let us consider the reordered linear system such that F-variables come first

$$\mathbf{A}\mathbf{u} = \begin{pmatrix} \mathbf{A}_{FF} & \mathbf{A}_{FC} \\ \mathbf{A}_{CF} & \mathbf{A}_{CC} \end{pmatrix} \begin{pmatrix} \mathbf{u}_F \\ \mathbf{u}_C \end{pmatrix} = \begin{pmatrix} \mathbf{f}_F \\ \mathbf{f}_C \end{pmatrix} = \mathbf{f} \enspace .$$

(Those variables which are to be contained in the coarse grid are commonly referred to as C-variables whereas the complementary set is related to the F-variables.) The *optimal* (but usually impractical!) prolongation $\widetilde{\mathbf{P}}$ is based on an exact solution of the homogeneous F-equations leading to

$$\widetilde{\mathbf{P}} = \begin{pmatrix} -\mathbf{A}_{FF}^{-1}\mathbf{A}_{FC} \\ \mathbf{I}_{CC} \end{pmatrix} \enspace .$$

Optimal means that the resulting Galerkin coarse grid operator $\mathbf{A}_c = \widetilde{\mathbf{P}}^T\mathbf{A}\widetilde{\mathbf{P}}$ equals the Schur complement.

Similarly, the *optimal* relaxation $\widetilde{\mathbf{S}}$ is based on an exact solution of the F-equations as well, yielding

$$\widetilde{\mathbf{S}} = \begin{pmatrix} 0 & -\mathbf{A}_{FF}^{-1}\mathbf{A}_{FC} \\ 0 & \mathbf{I}_{CC} \end{pmatrix} \enspace . \tag{1}$$

Hence, in the limit case of an optimal (but usually impractical) choice of $\mathbf{P}$ and $\mathbf{S}$ this means that

$$\widetilde{\mathbf{S}}\mathbf{b} = \widetilde{\mathbf{P}}\mathbf{b}_C \tag{2}$$

holds for an arbitrary vector $\mathbf{b} = \begin{pmatrix}\mathbf{b}_F & \mathbf{b}_C\end{pmatrix}^T$. In other words, the range of the relaxation and the range of the prolongation coincide:

$$\mathcal{R}(\widetilde{\mathbf{S}}) = \mathcal{R}(\widetilde{\mathbf{P}}) \ .$$

In this paper we present a formalism for the construction of proper prolongation operators in order to accomplish the transfer from coarse to fine grids within a multigrid algorithm. The main idea is to force relation (2) only locally (i.e. at each fine variable $\mathbf{i}$ that has to be interpolated) for a certain subset of (algebraically) smooth basis vectors $\mathbf{b}_k^{(\mathbf{i})}$ $(k = 1, \ldots, n_{\mathbf{P}}^{(\mathbf{i})})$. Depending on the particular choice of the basis vectors and the relaxation operator–which are applied to construct $\mathbf{P}$–classical operator-dependent prolongations can be recovered. Moreover, this rather general framework gives rise to many other variants whose complexity and accuracy can be controlled by a proper selection of basis vectors and smoothing operators. For example, geometric or other problem-dependent information can be easily exploited to tailor the prolongation to the particular application at hand. Note that the use of locally defined basis functions for the explicit construction of a multigrid component is closely related to and motivated by collocation coarse approximation in multigrid introduced in [14].

The explicit construction of $\mathbf{P}$ is specified in section 2. In section 3 numerical results for several two- and three-dimensional diffusion problems including jumping coefficients are presented. In particular a real-world three-dimensional image segmentation problem arising in medical applications is discussed. Finally, some conclusions are drawn in section 4.

2 Explicit construction of prolongation

2.1 Main idea

The main idea is to construct a more practical prolongation $\mathbf{P}$ by a certain local approximation of the governing equation (2). Since the construction of $\widetilde{\mathbf{S}}$ is much too costly in general, we have to apply a certain approximation. As a consequence, (2) will not be valid anymore for arbitrary $\mathbf{b}$. Hence, relation (2) is only forced for a certain set of (algebraically) smooth basis functions $\mathbf{b}_k^{(\mathbf{i})}$ and an approximate variant $\mathbf{S}$ of the optimal relaxation, i.e.,

$$\mathbf{S}_{\mathbf{i}}\mathbf{b}_k^{(\mathbf{i})} = \mathbf{P}_{\mathbf{i}}\left(\mathbf{b}_k^{(\mathbf{i})}\right)_C \qquad (k = 1, \ldots, n_{\mathbf{P}}^{(\mathbf{i})}) \ . \tag{3}$$

Here, the index $\mathbf{i}$ refers to the fine grid variable that is interpolated and $\mathbf{S}_{\mathbf{i}}$, $\mathbf{P}_{\mathbf{i}}$ refer to the $\mathbf{i}$th row of $\mathbf{S}$ and $\mathbf{P}$, respectively. Note that for different fine grid variables different basis functions may be applied.

2.2 Choosing the relaxation

We only consider F-relaxations, i.e., only F-variables are updated by the relaxation whereas the C-variables remain unchanged. Moreover, we want to approximate (1) by a much cheaper and much more *local* relaxation method. Locality is of particular importance in order to ensure a prolongation with a small "*radius*". An obvious choice is to use classical iterative methods based on a splitting $\mathbf{A}_{FF} = \mathbf{Q}_{FF} + (\mathbf{A}_{FF} - \mathbf{Q}_{FF})$, where $\mathbf{Q}_{FF}$ is an approximation for $\mathbf{A}_{FF}$ that can be easily inverted (like the diagonal or the upper/lower triangular part of $\mathbf{A}_{FF}$). Then, (1) is approximated by

$$\mathbf{S} \,:\, \mathbf{u} \to \overline{\mathbf{u}} \qquad \text{with} \quad \mathbf{Q}_{FF}\overline{\mathbf{u}}_F + (\mathbf{A}_{FF} - \mathbf{Q}_{FF})\,\mathbf{u}_F + \mathbf{A}_{FC}\mathbf{u}_C = \mathbf{f}_F \quad \text{and} \quad \overline{\mathbf{u}}_C = \mathbf{u}_C \enspace .$$

Consequently, the relaxation operator reads

$$\mathbf{S} = \begin{pmatrix} \mathbf{S}_{FF} & (\mathbf{S}_{FF} - \mathbf{I}_{FF})\,\mathbf{A}_{FF}^{-1}\mathbf{A}_{FC} \\ 0 & \mathbf{I}_{CC} \end{pmatrix} \quad \text{with} \quad \mathbf{S}_{FF} = \mathbf{I}_{FF} - \mathbf{Q}_{FF}^{-1}\mathbf{A}_{FF} \enspace ,$$

compare with $\widetilde{\mathbf{S}}$ from (1).

To ensure a clear presentation we consider a simple example. Let us assume that the fine grid matrix $\mathbf{A}$ is represented by a common five-point star stencil (possibly modified at boundaries) often used in the discretization of two-dimensional diffusion operators:

$$\begin{bmatrix} & N_{\mathbf{i}} & \\ W_{\mathbf{i}} & C_{\mathbf{i}} & E_{\mathbf{i}} \\ & S_{\mathbf{i}} & \end{bmatrix}_h \qquad (\mathbf{i} = 1, \ldots, n) \enspace . \tag{4}$$

We assume for simplicity a square fine grid of mesh-size $h = 1/n_x = 1/n_y$ with $n_x = n_y$ even. After elimination of boundary conditions we end up with a linear system of $(n_x - 1) \times (n_y - 1) = n$ equations. We assume a lexicographic ordering of grid points. Then the eight direct fine grid neighbors of an inner grid point $\mathbf{i}$ have indices $\mathbf{i} - n_x$ (southwestern), $\mathbf{i} - n_x + 1$ (southern), $\mathbf{i} - n_x + 2$ (southeastern), $\mathbf{i} - 1$ (western), $\mathbf{i} + 1$ (eastern), $\mathbf{i} + n_x - 2$ (northwestern), $\mathbf{i} + n_x - 1$ (northern), and $\mathbf{i} + n_x$ (northeastern), see Figure 1. For the description of a typical nine-point interpolation,

$$\left] \begin{matrix} Nw_i^P & N_i^P & Ne_i^P \\ W_i^P & 1 & E_i^P \\ Sw_i^P & S_i^P & Se_i^P \end{matrix} \right[\enspace , \tag{5}$$

the direct neighbors of coarse and related co-located fine grid points specified above have to be taken into account. The weights from (5) assign the ratio of the coarse grid variable u_i^c that is distributed to the eight direct fine grid neighbors of the co-located fine grid variable $u_{\mathbf{i}}$ in the prolongation process. Obviously, all these direct neighbors are F-points. At C-point $u_{\mathbf{i}}$ the coarse grid correction is simply injected from u_i^c. Let us consider the construction of the western and eastern weights

$$W_i^P, \; E_{i-1}^P \qquad (i = 1, \ldots, n_c) \enspace ,$$

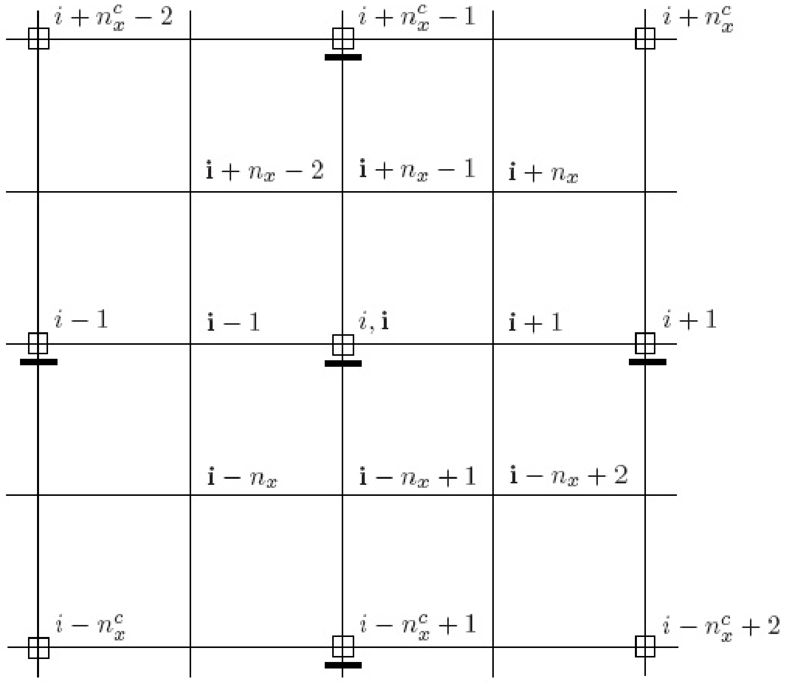

Figure 1: Direct neighbors of coarse grid point i and co-located fine grid point $\mathbf{i}$. Coarse variables (C-points) are marked by □.

compare with figure 2. An obvious choice for the related basis functions is

$$\mathbf{b}_1^{(\mathbf{i}-1)} \mathrel{\widehat{=}} 1 \ , \quad \mathbf{b}_2^{(\mathbf{i}-1)} \mathrel{\widehat{=}} x \ .$$

For simplicity, we apply Jacobi F-relaxation (FJAC)

$$\mathbf{S} = \begin{pmatrix} \mathbf{S}_{FF} & (\mathbf{S}_{FF} - \mathbf{I}_{FF})\, \mathbf{A}_{FF}^{-1}\mathbf{A}_{FC} \\ 0 & \mathbf{I}_{CC} \end{pmatrix} \qquad \text{with} \quad \mathbf{S}_{FF} = \mathbf{I}_{FF} - \mathbf{D}_{FF}^{-1}\mathbf{A}_{FF}$$

as an approximation for the optimal relaxation $\widetilde{\mathbf{S}}$ with $\widetilde{\mathbf{S}}_{FF} = 0$. Here $\mathbf{D}_{FF}$ denotes the diagonal part of $\mathbf{A}_{FF}$. Without loss of generality we set mesh size $h = 1$ and shift the origin to coarse grid point i. Then, the two basis functions $\{1, x\}$ restricted to the subdomain relevant to $\mathbf{P}_{\mathbf{i}-1}$ and reshaped to $2D$ form read in stencil notation

$$\begin{bmatrix} 1 & 1 & 1 \\ \underline{\mathbf{1}} & 1 & \underline{\mathbf{1}} \\ 1 & 1 & 1 \end{bmatrix}_h \ , \qquad \begin{bmatrix} -2 & -1 & 0 \\ \underline{\mathbf{-2}} & -1 & \underline{\mathbf{0}} \\ -2 & -1 & 0 \end{bmatrix}_h \ .$$

Elements corresponding to the interpolatory set of coarse variables are written in boldface and underlined. Now, the governing equations $\mathbf{S}_{\mathbf{i}-1}\mathbf{b}_k^{(\mathbf{i}-1)} = \mathbf{P}_{\mathbf{i}-1}\left(\mathbf{b}_k^{(\mathbf{i}-1)}\right)_C$ $(k = 1, 2)$ reduce

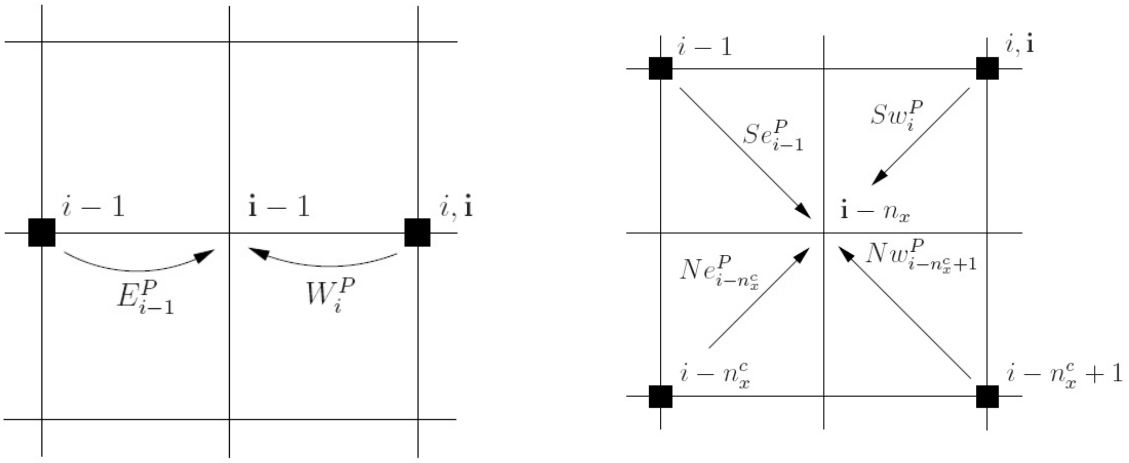

Figure 2: Interpolatory sets marked by ■ and prolongation weights for the western $(\mathbf{i}-1)$ and southwestern $(\mathbf{i}-n_x)$ neighbor of a co-located fine grid variable $\mathbf{i}$.

to

$$-\frac{1}{C_{\mathbf{i}-1}}\left(W_{\mathbf{i}-1}+E_{\mathbf{i}-1}+S_{\mathbf{i}-1}+N_{\mathbf{i}-1}\right) = 1\cdot E^P_{i-1}+1\cdot W^P_i \quad ,$$
$$\frac{1}{C_{\mathbf{i}-1}}\left(2W_{\mathbf{i}-1}+S_{\mathbf{i}-1}+N_{\mathbf{i}-1}\right) = -2\cdot E^P_{i-1}+0\cdot W^P_i$$

giving

$$W^P_i = -\frac{2E_{\mathbf{i}-1}+S_{\mathbf{i}-1}+N_{\mathbf{i}-1}}{2C_{\mathbf{i}-1}} \quad , \quad E^P_{i-1} = -\frac{2W_{\mathbf{i}-1}+S_{\mathbf{i}-1}+N_{\mathbf{i}-1}}{2C_{\mathbf{i}-1}} \quad .$$

Similar simple formulas result for the remaining prolongation weights using $\{1,y\}$ and $\{1,x,y,xy\}$ as basis functions. We denote the resulting prolongation method by FJAC-prolongation.

A better approximation of $\widetilde{\mathbf{S}}$, i.e. an improved approximation of $\widetilde{\mathbf{S}}_{FF}=0$ by $\mathbf{S}_{FF}$ should yield an improved $\mathbf{P}$. This gives rise to FGS-prolongation where we use interpolated values of the basis vectors for fine grid points that are located between two coarse grid points, compare with the left picture of figure 2. For basis functions $\{1,x\}$ and $\{1,y\}$ this is equivalent to approximating $\widetilde{\mathbf{S}}$ by Gauss-Seidel F-relaxation due to the governing equations

$$\mathbf{S}_{\mathbf{i}-1}\mathbf{b}_k^{(\mathbf{i}-1)} = \mathbf{P}_{\mathbf{i}-1}\left(\mathbf{b}_k^{(\mathbf{i}-1)}\right)_C \quad .$$

Finally, please note that in particular $\mathbf{S}_{FF}$ should be a good approximation for $\widetilde{\mathbf{S}}_{FF}$ w.r.t. the smooth basis vectors. To meet this requirement—which should lead to a further improvement of the resulting prolongation—we introduce a relaxation parameter $\omega^{(\mathbf{i})}$ such that

$$\left(\mathbf{S}_{FF}(\omega^{(\mathbf{i})})\right)_{\mathbf{i}}\left(\mathbf{b}_1^{(\mathbf{i})}\right)_F = \left(\widetilde{\mathbf{S}}_{FF}\right)_{\mathbf{i}}\left(\mathbf{b}_1^{(\mathbf{i})}\right)_F = 0 \tag{6}$$

with $\mathbf{b}_1^{(\mathbf{i})}=1$. For a compact 5-point stencil one obtains for the computation of W^P_i and E^P_{i-1}

$$\omega^{(\mathbf{i}-1)} = \frac{C_{\mathbf{i}-1}}{C_{\mathbf{i}-1}+S_{\mathbf{i}-1}+N_{\mathbf{i}-1}} \quad .$$

It is interesting to note, that the related ω-FGS prolongation is equivalent to black box prolongation [4] in case of 5-point stencils.

2.3 Canonical basis functions

The calculation of the non-zero entries of $\mathbf{P_i}$ obviously necessitates the solution of a small linear system

$$\left(\mathbf{M}^{(\mathbf{i})}\right)^T \mathbf{v}^{(\mathbf{i})} = \left(\mathbf{S_i}\mathbf{B}^{(\mathbf{i})}\right)^T$$

where

$$\mathbf{B}^{(\mathbf{i})} = \left[\mathbf{b}_1^{(\mathbf{i})}\,\mathbf{b}_2^{(\mathbf{i})}\,\ldots\,\mathbf{b}_{n_{\mathbf{P}}^{(\mathbf{i})}}^{(\mathbf{i})}\right]$$

denotes the matrix of size $(n \times n_{\mathbf{P}}^{(\mathbf{i})})$, whose columns are the basis vectors, and

$$\mathbf{M}^{(\mathbf{i})} = \hat{\mathbf{R}}\mathbf{B}^{(\mathbf{i})}\,, \tag{7}$$

denotes the $(n_{\mathbf{P}}^{(\mathbf{i})} \times n_{\mathbf{P}}^{(\mathbf{i})})$ matrix whose columns are obtained by restricting the basis vectors to the coarse grid and then sampling them on the interpolatory set of coarse variables. The solution of this linear systems for the computation of $\mathbf{P_i}$ can be avoided by canonical basis functions (CBFs) (as introduced in [14])

$$\bar{\mathbf{B}}^{(\mathbf{i})} := \mathbf{B}^{(\mathbf{i})}\left(\mathbf{M}^{(\mathbf{i})}\right)^{-1}$$

leading to $\left(\bar{\mathbf{M}}^{(\mathbf{i})}\right)^T = \hat{\mathbf{R}}\bar{\mathbf{B}}^{(\mathbf{i})} = \mathbf{I}$ where $\mathbf{I}$ denotes the $(n_{\mathbf{P}}^{(\mathbf{i})} \times n_{\mathbf{P}}^{(\mathbf{i})})$-identity matrix. This gives $\mathbf{v}^{(\mathbf{i})} = \left(\mathbf{S_i}\bar{\mathbf{B}}^{(\mathbf{i})}\right)^T$. Hence, the prolongation weights are simply obtained by applying a relaxation operator to a proper CBF. For example, the canonical form of $\{1, x\}$ turn out to be

$$\begin{bmatrix} 1 & 0.5 & 0 \\ \underline{\mathbf{1}} & 0.5 & \underline{\mathbf{0}} \\ 1 & 0.5 & 0 \end{bmatrix}_h \quad , \quad \begin{bmatrix} 0 & 0.5 & 1 \\ \underline{\mathbf{0}} & 0.5 & \underline{\mathbf{1}} \\ 0 & 0.5 & 1 \end{bmatrix}_h \quad .$$

Please note that the use of CBFs not only helps to save computational work but also leads to a very simple and convenient way for the implementation of the related prolongation operators.

2.4 Algebraic framework

For clarity, we so far described the construction of the prolongation only for a simple example. However, this can be easily generalized to an algebraic setting. Let us define the neighborhood of point $\mathbf{i}$ by

$$\Omega^{(\mathbf{i})} = \{\mathbf{j} \,:\, \mathbf{j} \neq \mathbf{i},\;\; \mathbf{A_{ij}} \neq 0\}\;\;.$$

This neighborhood may be split into a set of C- and a set of F-variables:

$$\Omega_C^{(\mathbf{i})} = \{\mathbf{j} \in \Omega^{(\mathbf{i})} \text{ and } \mathbf{j} \text{ is a } C\text{-point}\}\;\;,\quad \Omega_F^{(\mathbf{i})} = \{\mathbf{j} \in \Omega^{(\mathbf{i})} \text{ and } \mathbf{j} \text{ is an } F\text{-point}\}\;\;.$$

Considering a 5-point stencil the neighborhood of $\mathbf{i}$ reads

$$\Omega^{(\mathbf{i})} = \Omega_C^{(\mathbf{i})} \cup \Omega_F^{(\mathbf{i})} \quad \text{with} \quad \Omega_C^{(\mathbf{i})} = \{\mathbf{i}-1, \mathbf{i}+1\} \quad \text{and} \quad \Omega_F^{(\mathbf{i})} = \{\mathbf{i} - n_x + 1, \mathbf{i} + n_x - 1\} \ ,$$

compare with figure 1. Moreover, the (prescribed) set of interpolatory coarse variables that participate in the prolongation is denoted by $\Omega_{\mathbf{P}}^{(\mathbf{i})}$. For example, the interpolatory set for fine grid point $\mathbf{i}-1$ from figure 2 is given by $\Omega_{\mathbf{P}}^{(\mathbf{i}-1)} = \{\mathbf{i}-2, \mathbf{i}\}$.

Now, the calculation of prolongation weights—including an optimized relaxation parameter as introduced above—is carried out in two steps:

1. In a first step we consider those F-points which can be interpolated based on *direct* connections, i.e., $\Omega_C^{(\mathbf{i})} \cap \Omega_{\mathbf{P}}^{(\mathbf{i})} \neq \emptyset$. If $\Omega^{(\mathbf{i})} = \Omega_C^{(\mathbf{i})}$ (i.e., the neighborhood of $\mathbf{i}$ only consists of C-points) then Jacobi F-relaxation should be applied which is then obviously equivalent to the optimal relaxation $\widetilde{\mathbf{S}}$. For $\Omega^{(\mathbf{i})} \neq \Omega_C^{(\mathbf{i})}$ (and $\Omega_C^{(\mathbf{i})} \cap \Omega_{\mathbf{P}}^{(\mathbf{i})} \neq \emptyset$) we use $\omega^{(\mathbf{i})}$-Jacobi F-relaxation where the choice of the damping parameter is governed by (6). Since we have only one degree of freedom (the damping parameter $\omega^{(\mathbf{i})}$), we apply the constant, i.e., $\mathbf{b}_1^{(\mathbf{i})} \equiv 1$, to calculate the damping parameter from relation (6). This gives

$$\begin{aligned} (\mathbf{S}_{FF})_{\mathbf{i}} \left(\mathbf{b}_1^{(\mathbf{i})}\right)_F &= \left(1 - \omega^{(\mathbf{i})}\right) - \frac{\omega^{(\mathbf{i})}}{\mathbf{A_{ii}}} \sum_{\mathbf{j} \in \Omega^{(\mathbf{i})} \setminus \Omega_C^{(\mathbf{i})}} \mathbf{A_{ij}} = 0 \\ \Leftrightarrow \quad \omega^{(\mathbf{i})} &= \frac{\mathbf{A_{ii}}}{\mathbf{A_{ii}} + \sum_{\mathbf{j} \in \Omega^{(\mathbf{i})} \setminus \Omega_C^{(\mathbf{i})}} \mathbf{A_{ij}}} \ . \end{aligned} \tag{8}$$

   Note that $\omega^{(\mathbf{i})}$ is well-defined in the "common case" where we have $\mathbf{A_{ii}} = -\sum_{\mathbf{j} \in \Omega^{(\mathbf{i})}} \mathbf{A_{ij}}$ due to $\Omega_C^{(\mathbf{i})} \neq \emptyset$. Obviously (8) leads to *overrelaxation* (i.e. $\omega^{(\mathbf{i})} \geq 1$) in the common case. This is not surprising since the damping parameter has been tailored w.r.t. a *smooth* error component and not w.r.t. the *non-smooth* error components (where we know that usually underrelaxation is the method of choice). If $\Omega^{(\mathbf{i})} = \Omega_C^{(\mathbf{i})}$, then (8) yields $\omega^{(\mathbf{i})} = 1$ which is consistent with the above statement that in this case Jacobi F-relaxation without damping should be carried out. Hence, in principle we do not have to distinguish between these cases which is helpful w.r.t. an efficient implementation.

2. In a second step we consider those F-points $\mathbf{i}$ which do not have a direct C-connectivity, that is $\Omega_C^{(\mathbf{i})} \cap \Omega_{\mathbf{P}}^{(\mathbf{i})} = \emptyset$. Note, that a direct application of damped Jacobi F-relaxation might not be appropriate for these points because the "*optimal*" damping parameter as derived in (8) might not be well-defined in this case since the denominator becomes zero if $\Omega_C^{(\mathbf{i})} = \emptyset$ (which is the usual case when there is no direct C-connectivity). Instead we proceed as follows. Whenever possible we replace the values in $\Omega_F^{(\mathbf{i})}$ by their interpolated values based on direct connections as described in the first step above. These values are collected in the set $\Omega_D^{(\mathbf{i})} \subset \Omega_F^{(\mathbf{i})}$. Note that the union of the direct connections that interpolate the variables from $\Omega_D^{(\mathbf{i})}$ constitute the set of interpolatory variables $\Omega_{\mathbf{P}}^{(\mathbf{i})}$.

After this preparatory step we can proceed as in the case of direct C-connectivity. If $\Omega_D^{(\mathbf{i})} = \Omega_F^{(\mathbf{i})}$ we simply apply undamped F-relaxation which leads to $(S_{FF})_{\mathbf{i}} = 0$. If $\Omega_D^{(\mathbf{i})} \neq \Omega_F^{(\mathbf{i})}$ (but of course $\Omega_D^{(\mathbf{i})} \cap \Omega_F^{(\mathbf{i})} \neq \emptyset$, since any reasonable coarsening should ensure at least "*strong* F-neighbors", if no direct C-connectivity can be accomplished) we use $\omega^{(\mathbf{i})}$-Jacobi F-relaxation with

$$\omega^{(\mathbf{i})} = \frac{\mathbf{A_{ii}}}{\mathbf{A_{ii}} + \sum_{\mathbf{j} \in \Omega_F^{(\mathbf{i})} \setminus \Omega_D^{(\mathbf{i})}} \mathbf{A_{ij}}} \quad . \tag{9}$$

Please note again that for $\Omega_D^{(\mathbf{i})} = \Omega_F^{(\mathbf{i})}$ eq.(9) yields $\omega^{(\mathbf{i})} = 1$, so in principle we do not have to treat this case separately.

We would like to point out that in our example the weights in x- and y-direction have to be calculated according to step 1, whereas the "diagonal" weights have to be computed following step 2, c.f. figure 2. The resulting prolongation refers to ω-FGS prolongation.

3 Numerical experiments

3.1 Interface problems

We consider the two-dimensional diffusion equation on the unit square with Dirichlet boundary conditions

$$\begin{aligned} -\left(a(x,y)\, u_x(x,y) \right)_x - \left(b(x,y)\, u_y(x,y) \right)_y &= f(x,y) \quad , \\ u(x,y) &= g(x,y) \quad . \end{aligned}$$

We use a finite volume discretization with fine grid mesh size $h = 1/64$ and a random initial guess. In all our numerical tests the following multigrid components are kept fixed: 6 levels, V(1,1)-cycles, RB-JAC relaxation, Galerkin coarse grid approximation. In addition, we consider four different matrix-dependent prolongations: black box (BB), FJAC, FGS, and ω-FGS prolongation. The restriction is always selected as the transpose of the corresponding prolongation.

We consider five different testcases (**TC1 - TC5**):

TC1: Vertical jump,	**TC2**: Inhomogeneous strip,
TC3: Inhomogeneous square,	**TC4**: Inhomogeneous diamond,
TC5: Inhomogeneous staircase,	

The different choices for the diffusion coefficients a, b for **TC1 - TC5** are specified in Figures 3, 4, and 5. We use a random initial guess. Right hand side f and boundary condition g are set to zero in all test cases. Hence, the exact solution is known to be zero as well. In this way the numerical experiments are not limited by machine accuracy and we are able to determine

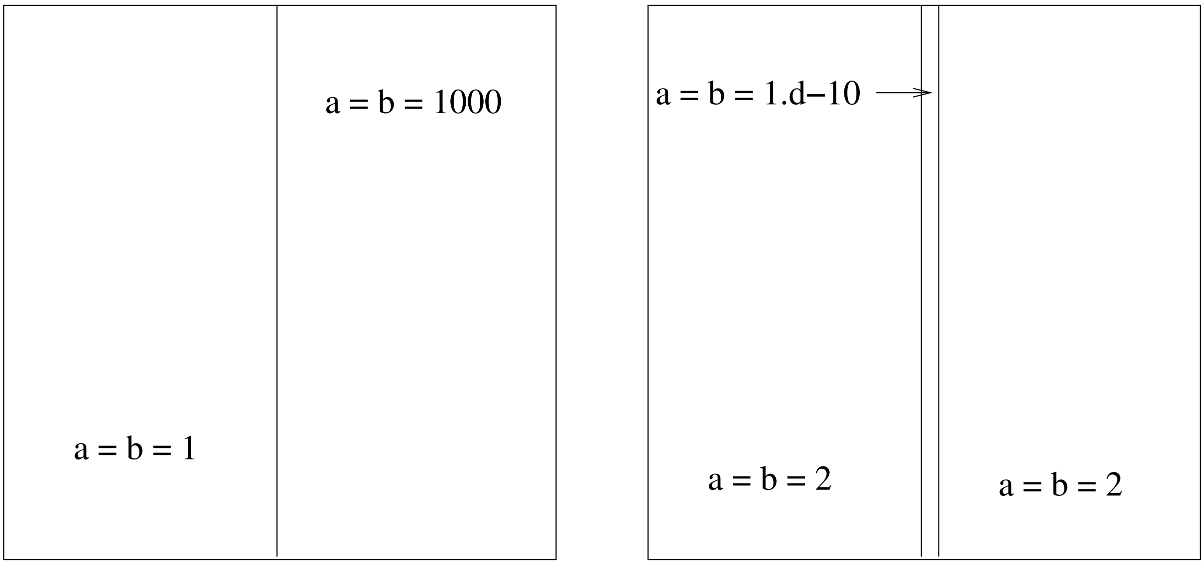

Fig. 3 (a) **TC1**.

Fig. 3 (b) **TC2**.

Figure 3: Distribution of diffusion coefficients a, b for **TC1**, **TC2**.

asymptotic convergence factors. The convergence histories for **TC1** - **TC5** for the different transfer operators are shown in figures 6 - 10.

ω-FGS prolongation and black box prolongation lead to the best multigrid algorithms. In fact, these two prolongations behave very similarly (note that they only coincide for 5-point stencils, but in the numerical experiments we deal with 9-point stencils on coarse grids due to the Galerkin coarse approximation). It is interesting to note that "improving the relaxation" (i.e. a better approximation of the optimal relaxation (1) by going from FJAC to ω-FGS relaxation) indeed leads to an improved prolongation. This is in good accordance with the main philosophy and motivation of our framework for the construction of prolongation operators.

3.2 Segmentation

The goal of image segmentation is to partition an image into two or more regions characterized by, e.g., similar intensity or texture in order to simplify image analysis. Practical applications include the location of tumors in medical data sets or objects in satellite images and face recognition.

We consider a variational approach for image segmentation based on linear anisotropic diffusion and related to random walks [6, 7]. In order to control the quality of the segmentation, the approach is half-automatic and especially useful for some applications in medical image segmentation [10].

First, the user, e.g., a physician, marks some points or regions as landmarks within a given

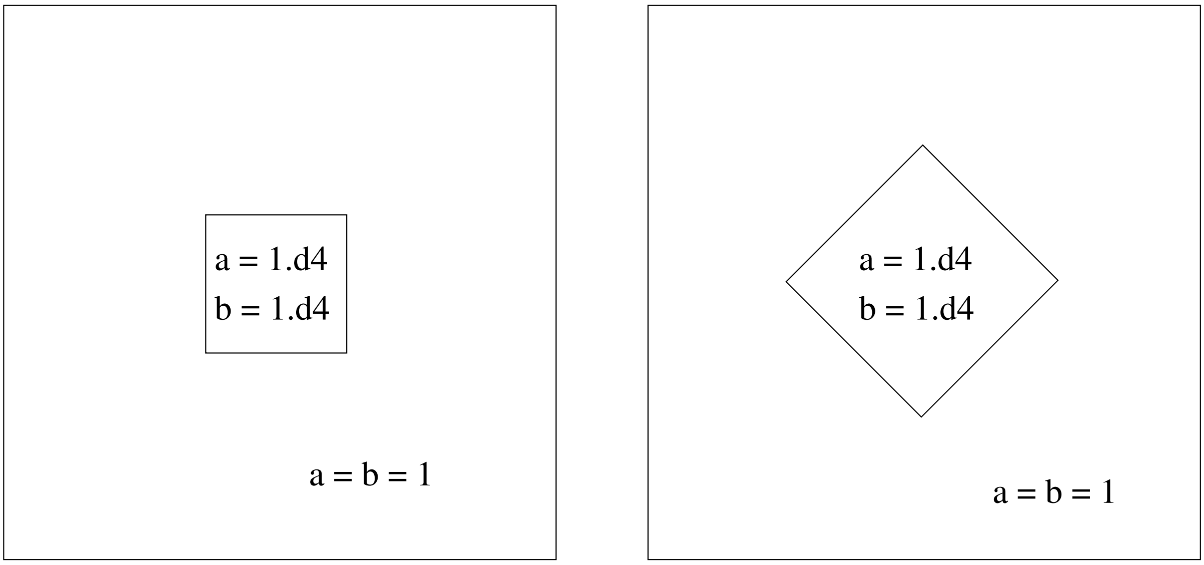

Fig. 4 (a) **TC3**.

Fig. 4 (b) **TC4**.

Figure 4: Distribution of diffusion coefficients a, b for **TC3**, **TC4**.

image, for which he knows, whether they belong to the object that is to be segmented. An example, where one point inside the eye is selected, can be found in figure 11. Dependent on this decision we assign them the value (probability) 1 or 0 whether being part of the segmented region. After that, an anisotropic linear diffusion described by

$$\begin{aligned} -\mathrm{div}\left(\begin{pmatrix} e^{-\beta(I_x)^2} & 0 \\ 0 & e^{-\beta(I_y)^2} \end{pmatrix} \nabla u\right) &= 0 \quad \text{if } \mathbf{x} \in \Omega \setminus \Omega_c \\ u &= u_0 \quad \text{if } \mathbf{x} \in \Omega_c \end{aligned} \tag{10}$$

spreads the information over the whole image domain Ω. Ω_c is the region of landmarks, $u_0 \in \{0, 1\}$ denotes the values at the landmark points, I_x, I_y are image derivatives in x and y direction computed by simple finite differences and β controls the jumps in the coefficients and thus how sharp edges will be in the segmentation result. The solution u itself can be thought of being the probability for each point $\mathbf{x} \in \Omega$ to belong to the segmented region. At the end it is binarized with threshold 0.5.

One example segmentation is depicted in figure 11 also found in [11], but now we do the computations for the whole 3D volume of size 444 × 448 × 20 and use the following multigrid components:

- V(2,1)-cycles with an alternating line Gauss-Seidel smoother,
- collocation coarse approximation (CCA) [14] for the computation of the coarse operators leading to 7-point coarse operators,
- and ω-FGS prolongation in 3D as described in the previous sections.

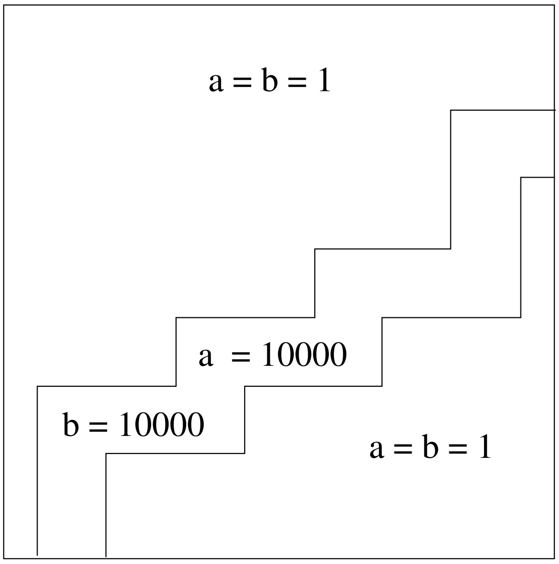

Figure 5: Distribution of diffusion coefficients a, b for **TC5**.

CCA is based on a similar philosophy than the presented prolongations: The coarse operator is selected such that

$$\mathbf{A}_c \left(\mathbf{b}_k^{(\mathbf{i})}\right)_C = \mathbf{R_i} \mathbf{A} \mathbf{b}_k^{(\mathbf{i})}$$

holds for certain basis vectors. Here, $\mathbf{R_i}$ refers to the $\mathbf{i}$th row of a fixed restriction operator $\mathbf{R}$. Details are given in [14].

Besides the fact that it is straight forward to extend the prolongation operators to 3D they can also be easily parallelized due to their locality. We chose to do a shared memory parallelization for the setup of the prolongation operators in order to be able to compute the transfers efficiently on a current multi-core architecture (Intel®Core™2 Quad 2.66 GHz, 4 MB L2 cache, 8 GB RAM) by OpenMP. The multigrid solver itself was not parallelized. Runtime results are found in table 1.

Table 1: Runtimes for segmentation of eye (size 444 × 448 × 20) split into setup time, solver time, and overall segmentation time, on 1 core and 4 cores of an Intel Core 2 Quad 2.66 GHz using $\beta = 80$ and 5 V(2,1)-cycles.

cores	setup	solver	segmentation
1	42.8 s	8.5 s	90.0 s
4	12.7 s	8.5 s	61.0 s

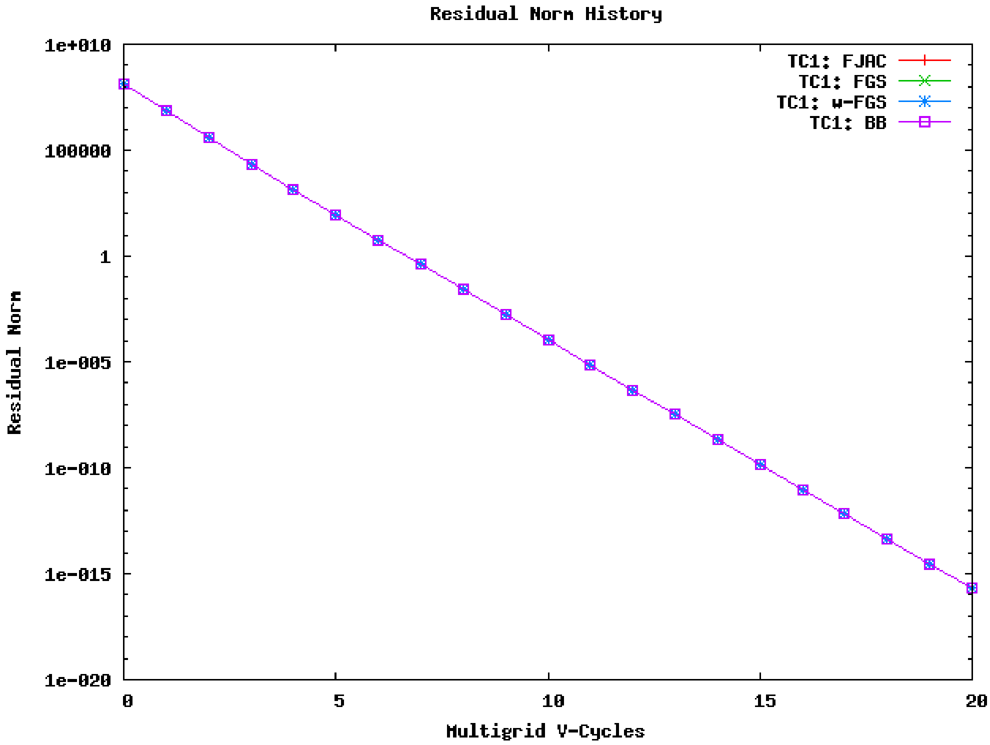

Figure 6: Convergence history for **TC1**: Vertical jump.

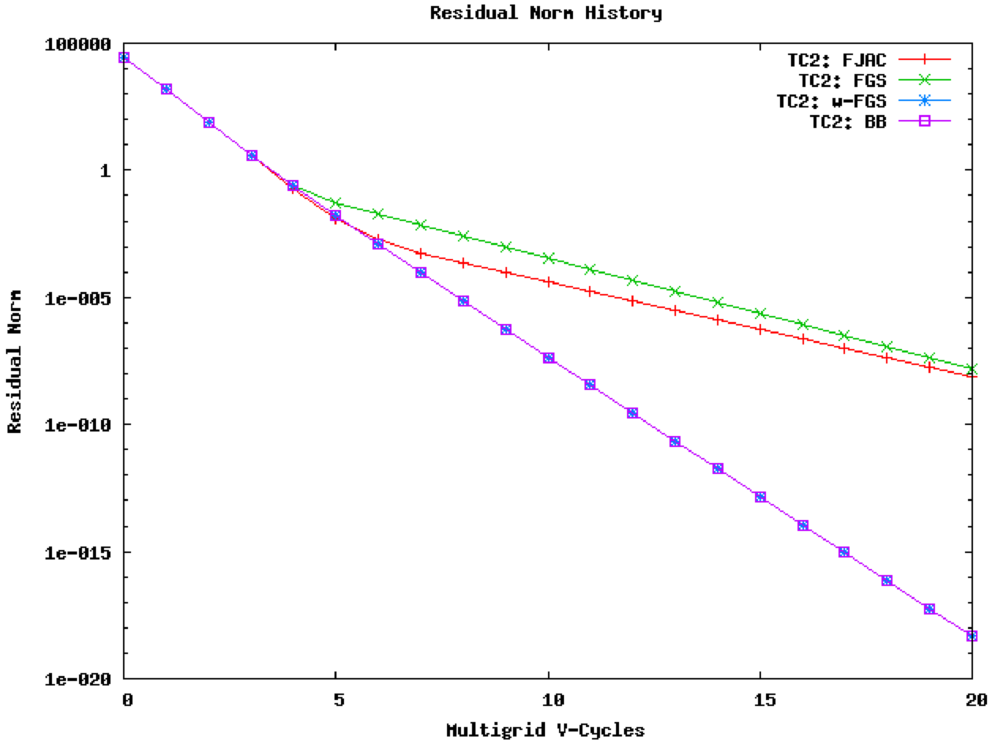

Figure 7: Convergence history for **TC2**: Inhomogeneous strip.

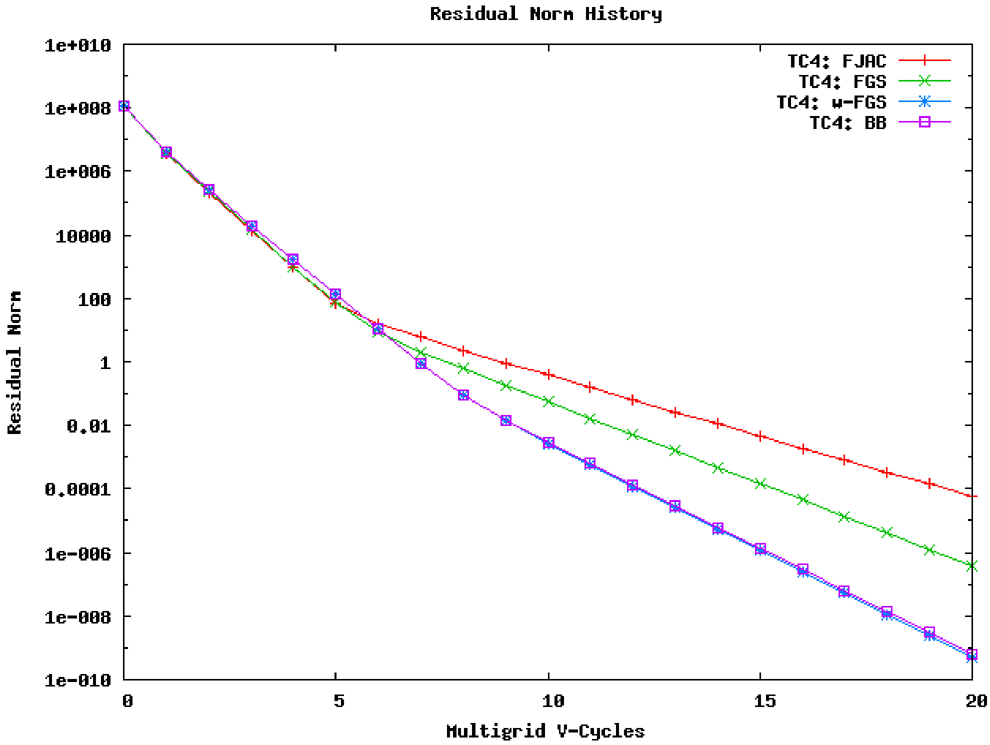

Figure 8: Convergence history for **TC3**: Inhomogeneous square.

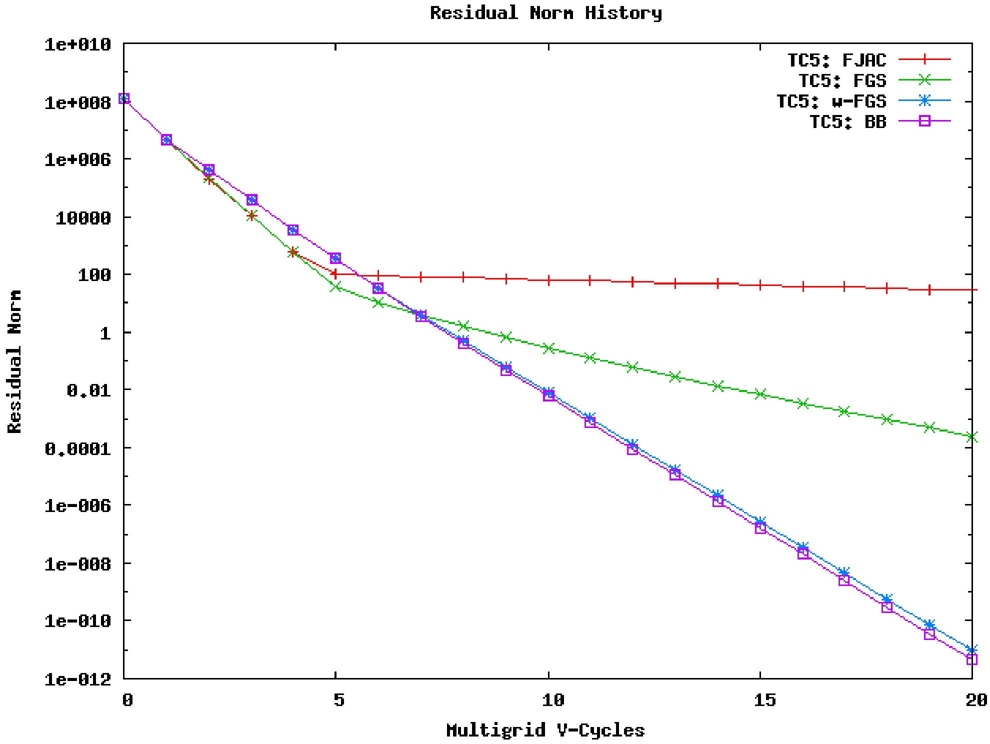

Figure 9: Convergence history for **TC4**: Inhomogeneous diamond.

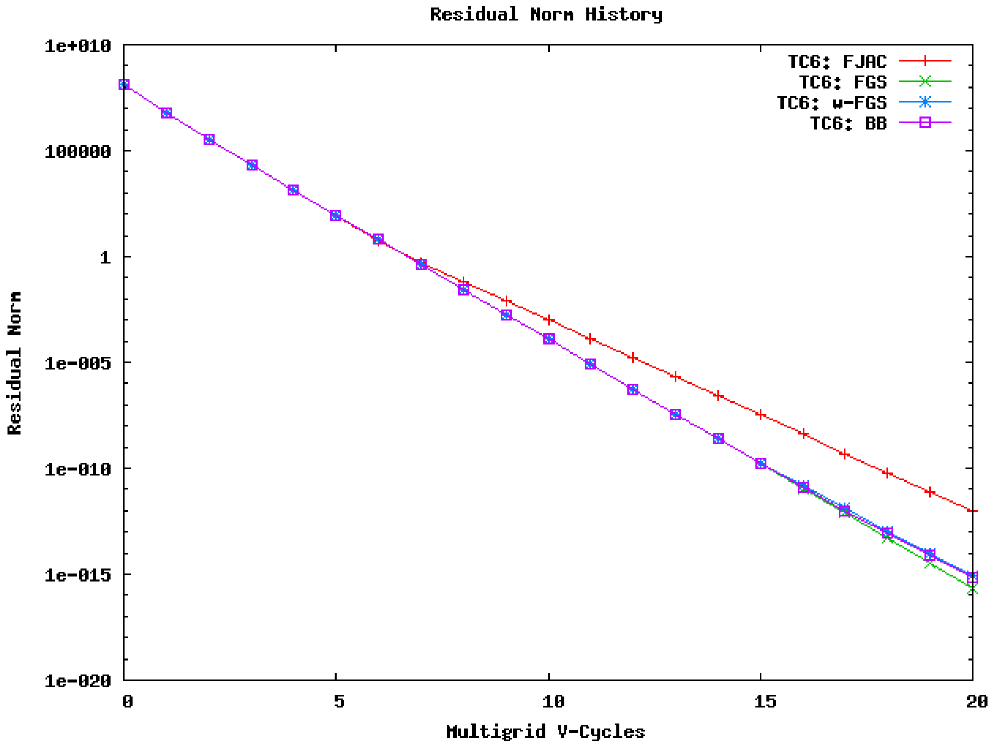

Figure 10: Convergence history for **TC5**: Inhomogeneous staircase.

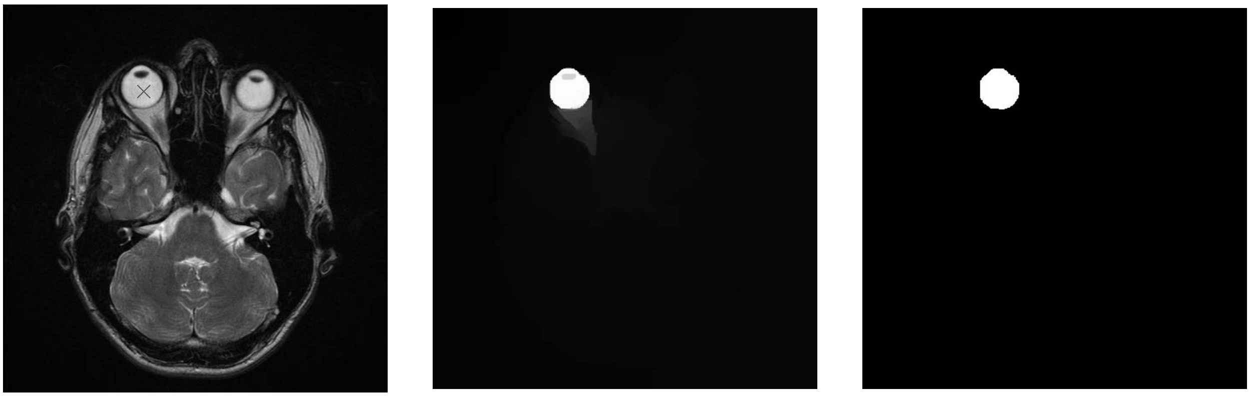

Figure 11: Segmentation of an eye out of a human head in an MRI volume of size 444 × 448 × 20 with one landmark in the middle of the eye and Dirichlet boundary conditions.

4 Conclusions and outlook

We presented a general framework formulated both for a geometric and an algebraic multigrid setting for the construction of prolongation operators, where classical matrix-dependent transfers can be recovered as special cases. The experiments showed that ω-FGS prolongation is as robust as black box prolongation while using less geometric information. Moreover, (precomputed) CBFs allow for a convenient and efficient implementation and parallelization. The prolongation weights are simply obtained by applying a relaxation operator to a proper CBF.

Next we want to make use of other relaxations and/or basis functions, in particular we will investigate a problem-dependent choice of relaxation and a problem-dependent and adaptive choice of basis functions. Furthermore, we plan to extend our approach to irregular grids and systems (the latter one being straight forward).

References

[1] A. Brandt, “Multi-level adaptive solutions to boundary-value problems,” *Mathematics of Computation*, vol. 31, pp. 333–390, 1977.

[2] ——, “1984 multigrid guide with applications to fluid dynamics,” Monograph, GMD-Studie 85, GMD-FIT, Postfach 1240, D-5205, St. Augustin 1, West Germany, 1985.

[3] W. L. Briggs, V. E. Henson, and S. F. McCormick, *A multigrid tutorial*, 2nd ed. Philadelphia: SIAM, 2000.

[4] J. E. Dendy (Jr.), “Black box multigrid,” *J. Comput. Phys.*, vol. 48, pp. 366–386, 1982.

[5] R. D. Falgout, “Introduction to algebraic multigrid,” *Computing in Science and Engineering*, vol. 8, no. 6, pp. 24–33, 2006.

[6] L. Grady, “Random Walks for Image Segmentation,” *IEEE Transactions on pattern analysis and machine intelligence*, vol. 28, no. 11, pp. 1768–1783, 2006.

[7] L. Grady, T. Tasdizen, and R. Whitaker, “A Geometric Multigrid Approach to Solving the 2D Inhomogeneous Laplace Equation with Internal Dirichlet Boundary Conditions,” *IEEE International Conference on Image Processing (ICIP)*, vol. 2, 2005.

[8] W. Hackbusch, *Multi-grid methods and applications.* Berlin: Springer, 1985.

[9] W. Hackbusch and U. Trottenberg, Eds., *Multigrid Methods.* Berlin: Springer-Verlag, 1982.

[10] J. Han, C. Bennewitz, H. Köstler, J. Hornegger, and T. Kuwert, "Computer-Aided Validation of Hybrid SPECT/CT Scanners," *Computerized Medical Imaging and Graphics*, vol. 32, no. 5, pp. 388–395, 2008.

[11] H. Köstler, *A Multigrid Framework for Variational Approaches in Medical Image Processing and Computer Vision.* Verlag Dr. Hut, München, 2008.

[12] U. Trottenberg, C. Oosterlee, and A. Schüller, *Multigrid.* London and San Diego: Academic Press, 2001.

[13] P. Wesseling, *An introduction to multigrid methods*, ser. Pure and Applied Mathematics. Chichester: John Wiley & Sons, 1992.

[14] R. Wienands and I. Yavneh, "Collocation coarse approximation (CCA) in multigrid," *Submitted to SIAM. J. Sci. Comput.*, 2008.

[15] I. Yavneh, "Why multigrid methods are so efficient," *Computing in Science and Engineering*, vol. 8, no. 6, pp. 12–22, 2006.